Reproduction, Fertility and Development, 2021, **33**(5), 328–337
https://doi.org/10.1071/RD20189_AC

Supplementary Material

Metabolomics analysis reveals metabolic changes associated with trans-resveratrol treatment in experimental cryptorchidism mice

Siqiang Li[A,*], *Yun Li*[A,B,*], *Fujia Chen*[A], *Yurong Yang*[A], *Li Song*[A], *Chaoying Liu*[A,B], *Baogen Wang*[A], *Yuanhong Xu*[A], *Mingguang Shao*[A] *and Enzhong Li*[A,C]

[A]School of Biological and Food Processing Engineering, Huanghuai University, Zhumadian, China.

[B]Zhumadian Academy of Industry Innovation and Development, Huanghuai University, Zhumadian, China.

[C]Corresponding author. Email: enzhongli@163.com

Fig. S1. PCA score plot of QC and metabolites collected from the control, cryptorchid, and RSV-treated cryptorchid group mice in both the (A) ESI+ and (B) ESI– modes.

Fig. S2. Multivariate statistical analyses of metabolites in the testis fragments of mice in the cryptorchid group versus the control group.

Fig. S3. Multivariate statistical analyses of metabolites in the testis fragments of mice in the RSV-treated cryptorchid group versus the cryptorchid group.

Fig. S4. Multivariate statistical analyses of metabolites in the testis fragments of mice in the RSV-treated cryptorchid group versus the control group.

Fig. S5. Histogram showed the common and unique differential metabolites in the control, cryptorchid, and RSV-treated cryptorchid groups.

Fig. S6. Differential metabolic pathways (Top 20) for cryptorchid group versus control group in ESI+ (A) and ESI– (B) modes.

Fig. S7. Differential metabolic pathways for RSV-treated cryptorchid group versus cryptorchid group in ESI+ (A) and ESI– (B) modes.

*These authors contributed equally to this work.

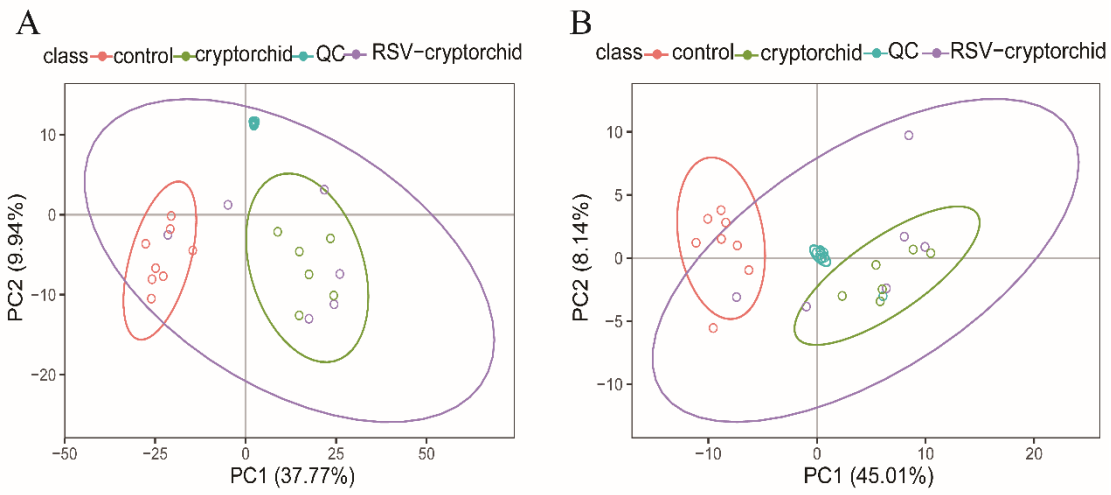

Fig. S1. PCA score plot of QC and metabolites collected from the control, cryptorchid, and RSV-treated cryptorchid group mice in both the (A) ESI+ and (B) ESI− modes.

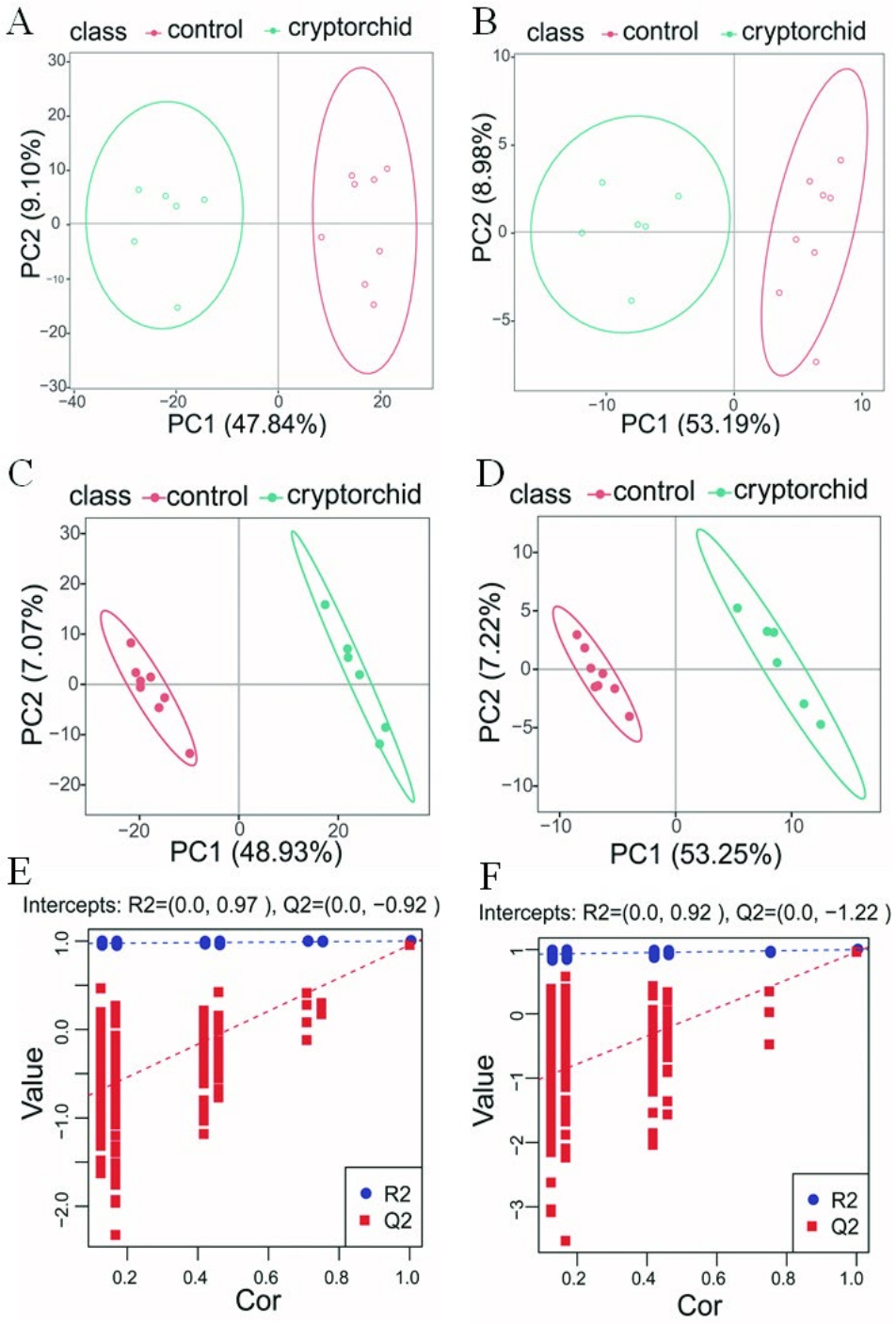

Fig. S2. Multivariate statistical analyses of metabolites in the testis fragments of mice in the cryptorchid group versus the control group. PCA score plots in the (A) ESI+ mode and (B) ESI– mode. PLS-DA score plots in the (C) ESI+ mode and (D) ESI– mode. Response sequencing check diagrams of PLS-DA models in the (E) ESI+ mode and (F) ESI– mode.

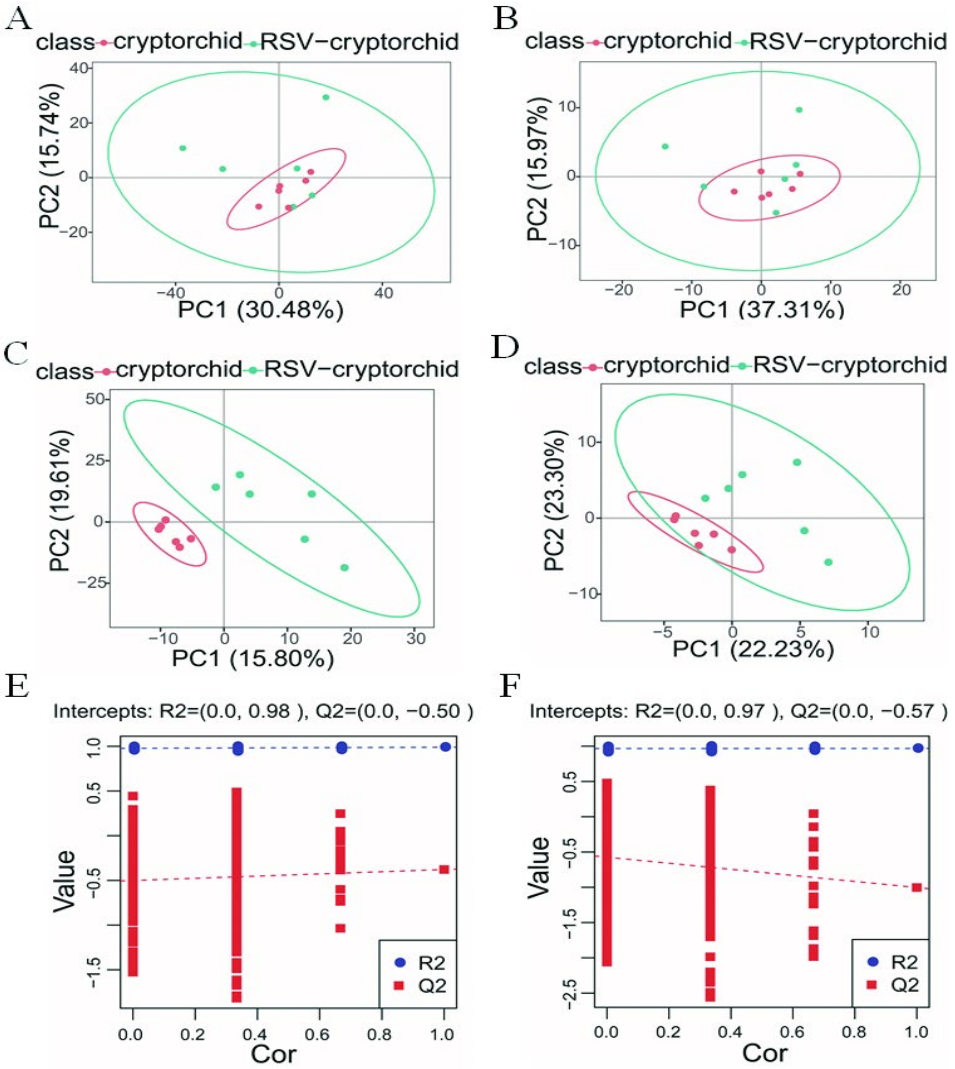

Fig. S3. Multivariate statistical analyses of metabolites in the testis fragments of mice in the RSV-treated cryptorchid group versus the cryptorchid group. PCA score plots in the (A) ESI+ mode and (B) ESI– mode. PLS-DA score plots in the (C) ESI+ mode and (D): ESI– mode. Response sequencing check diagrams of PLS-DA models in the (E) ESI+ mode and (F) ESI– mode.

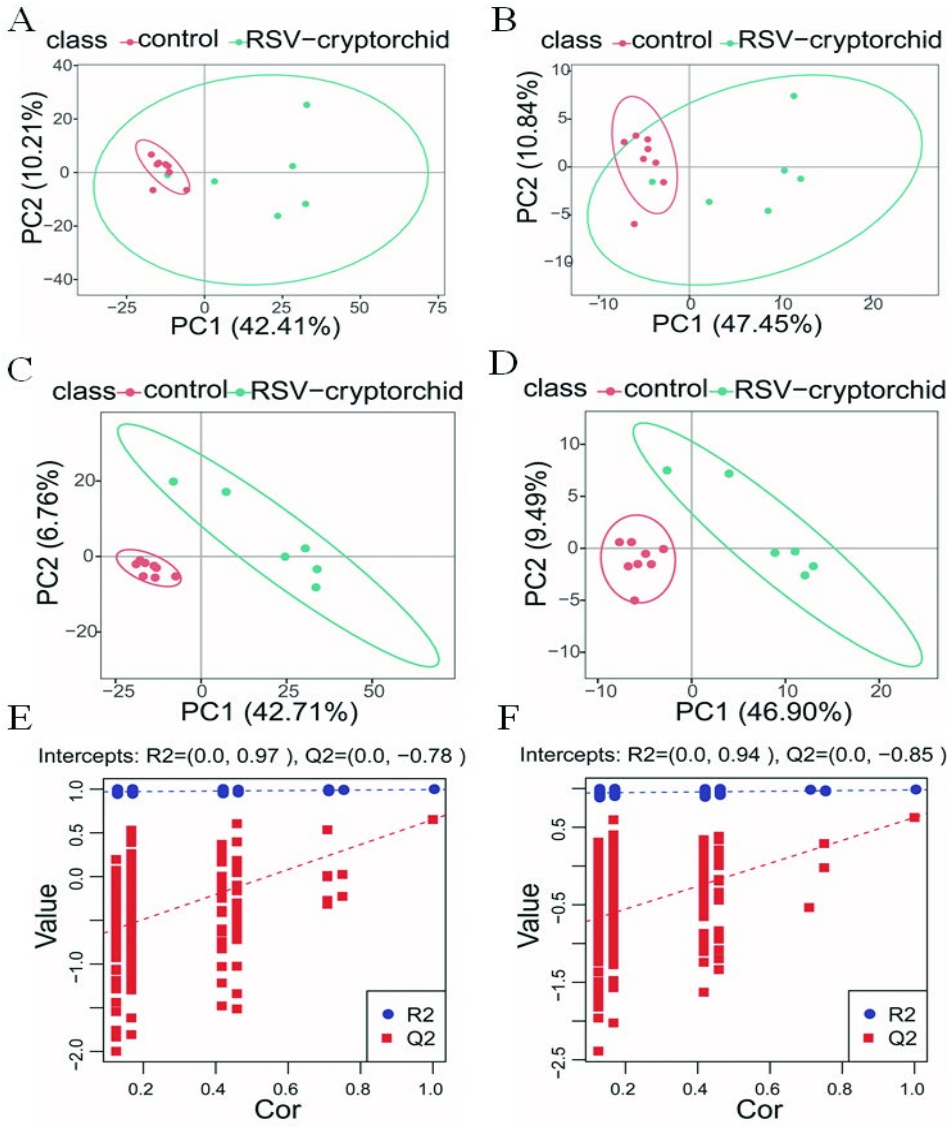

Fig. S4. Multivariate statistical analyses of metabolites in the testis fragments of mice in the RSV-treated cryptorchid group versus the control group. PCA score plots in the (A) ESI+ mode and (B) ESI− mode. PLS-DA score plots in the (C) ESI+ mode and (D) ESI− mode. Response sequencing check diagrams of PLS-DA models in the (E) ESI+ mode and (F) ESI− mode.

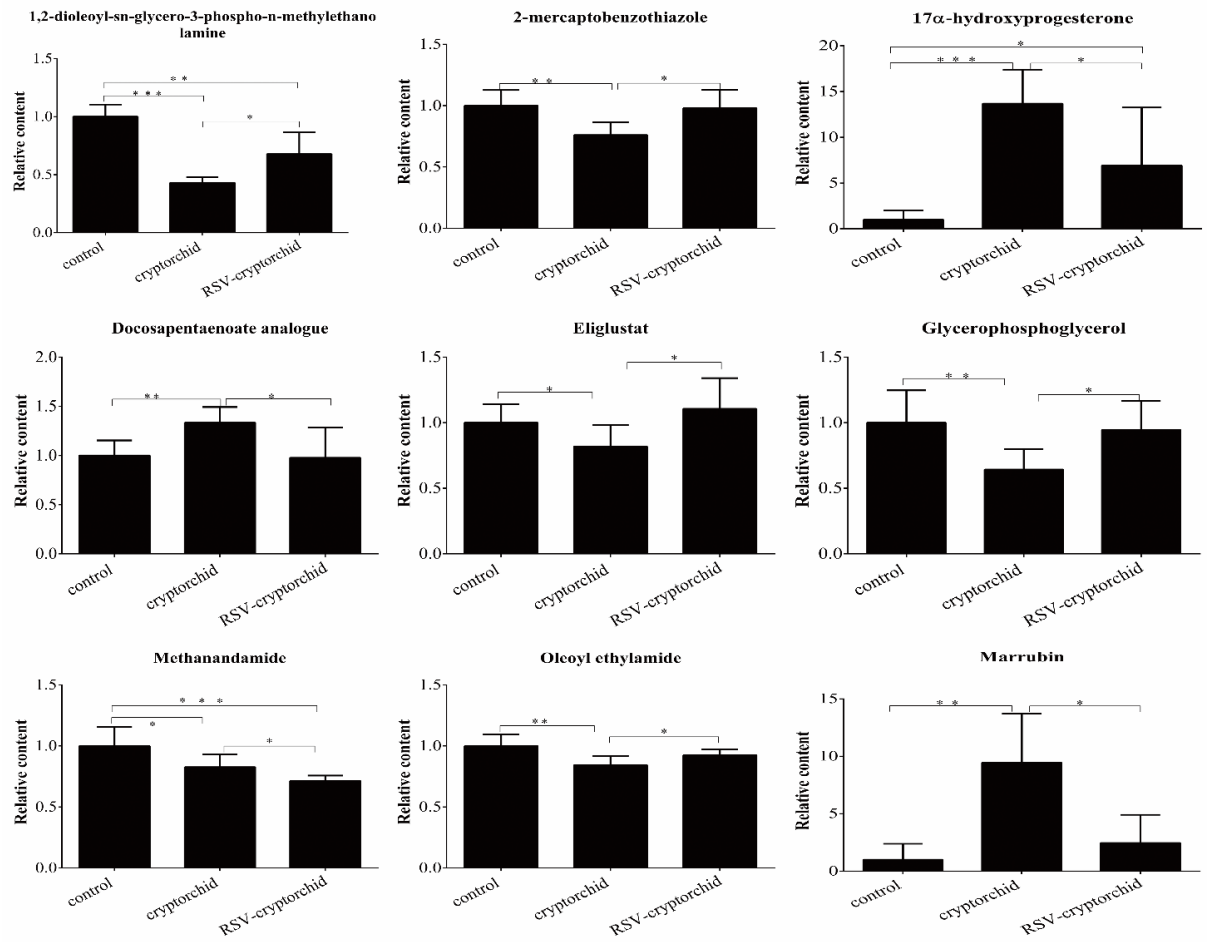

Fig. S5. Histogram showed the common and unique differential metabolites in the control, cryptorchid, and RSV-treated cryptorchid groups. Each value is mean ± s.d. $^{*}P < 0.05$, $^{**}P < 0.01$, and $^{***}P < 0.001$.

(*Fig. S5. continued over page*)

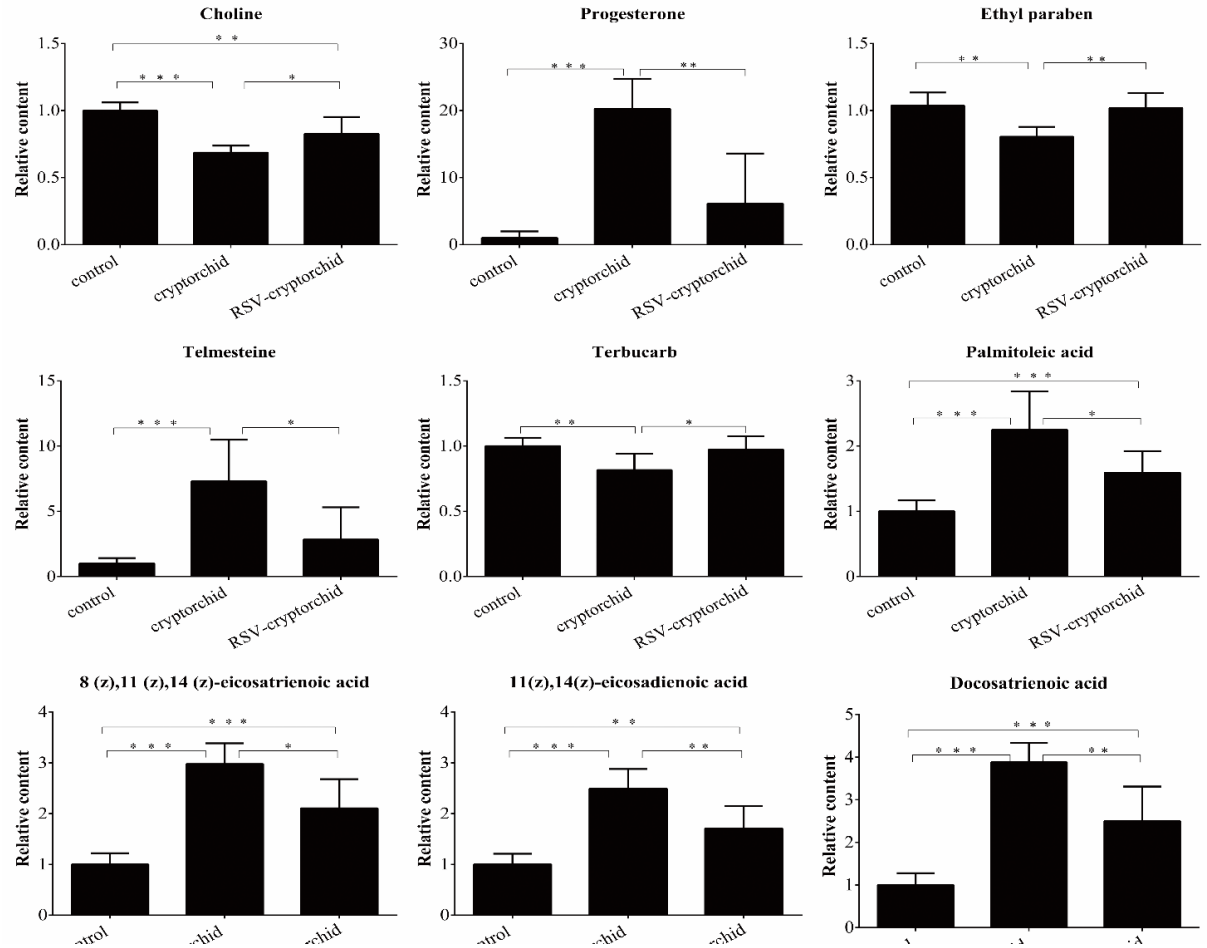
Choline
Progesterone
Ethyl paraben
Telmesteine
Terbucarb
Palmitoleic acid
8 (z),11 (z),14 (z)-eicosatrienoic acid
11(z),14(z)-eicosadienoic acid
Docosatrienoic acid
Relative content
control
cryptorchid
RSV-cryptorchid

Fig. S5. *cont.*

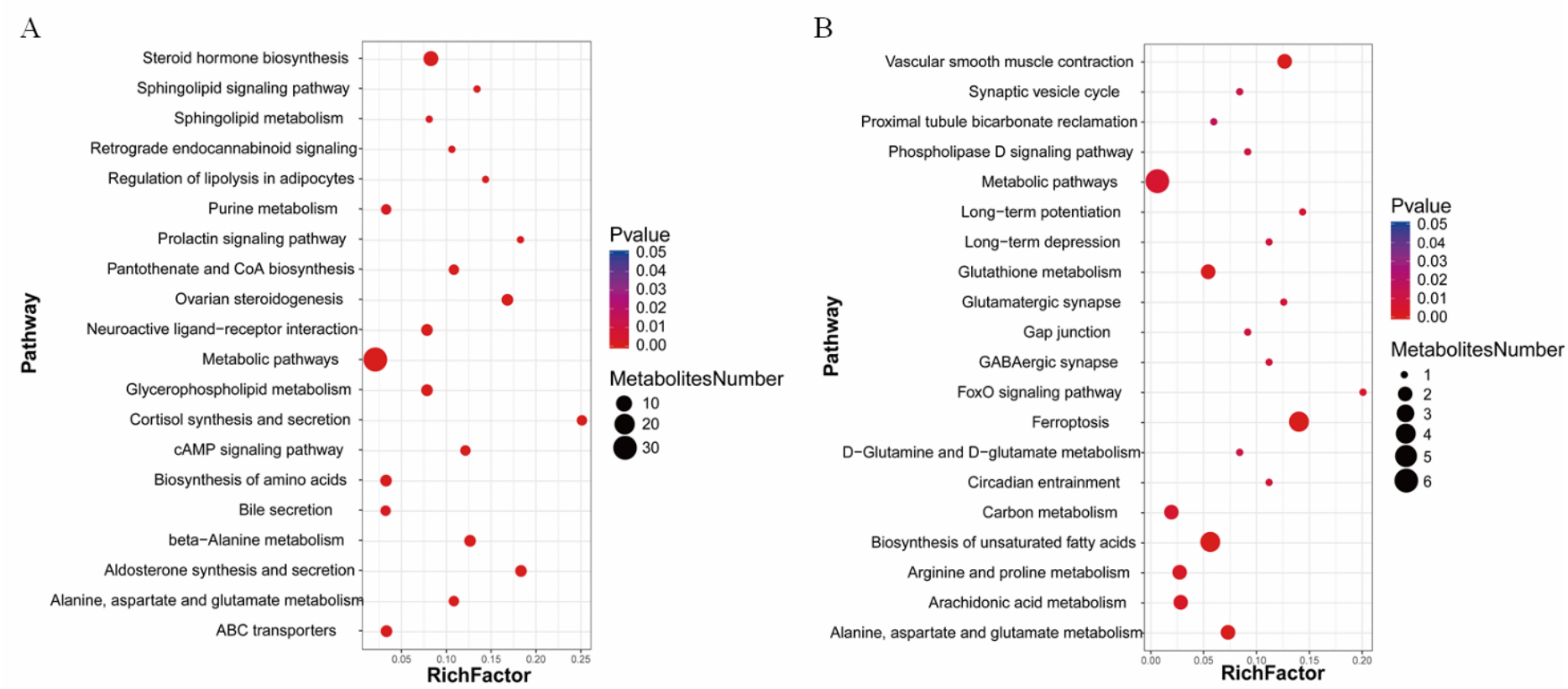

Fig. S6. Differential metabolic pathways (Top 20) for cryptorchid group versus control group in ESI+ (A) and ESI– (B) modes.

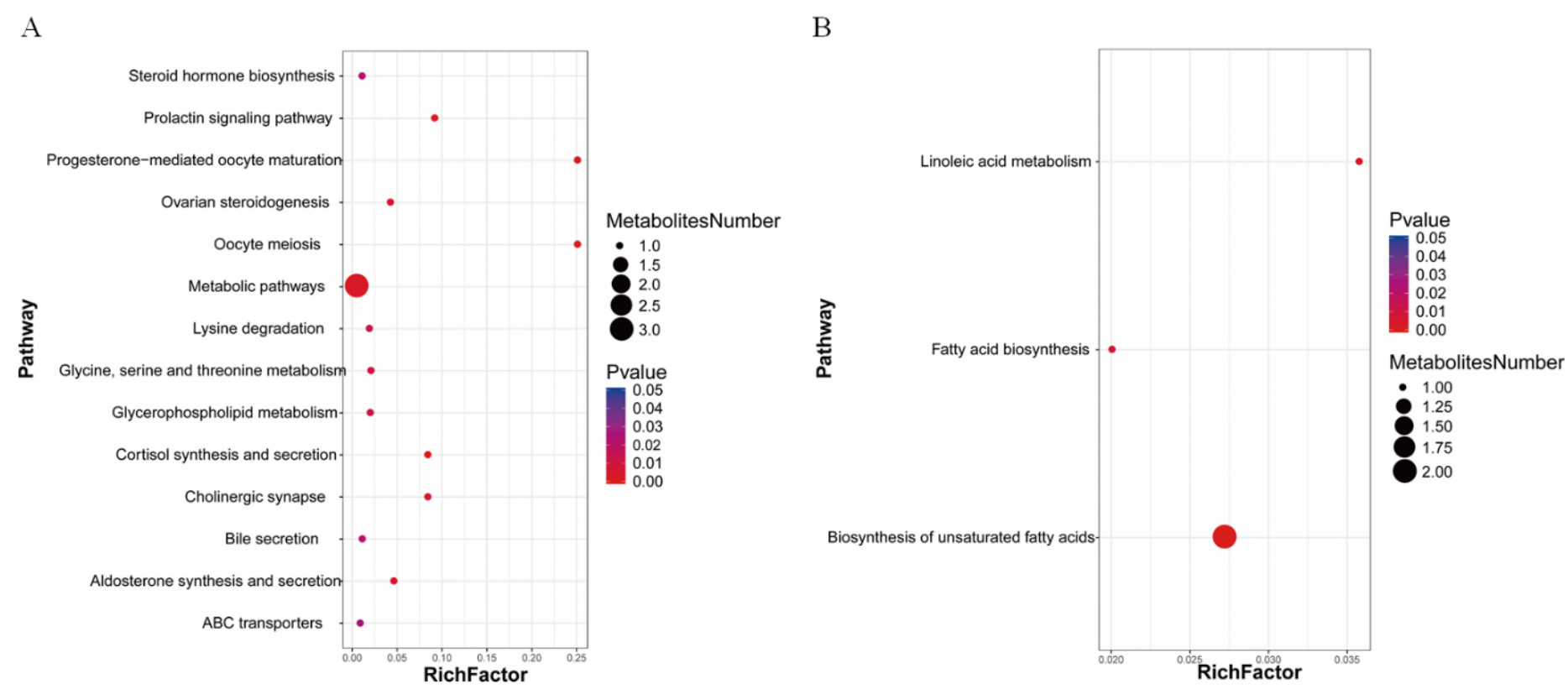

Fig. S7. Differential metabolic pathways for RSV-treated cryptorchid group versus cryptorchid group in ESI+ (A) and ESI– (B) modes.